

# Uniformity of the Large Beam of ELISE during Cs Conditioning

F. Bonomo<sup>a)</sup>, I. Mario, R. Nocentini, D. Wunderlich, U. Fantz and the NNBI-Team

*Max-Planck-Institut für Plasmaphysik, Boltzmannstr. 2, 85748 Garching, Germany*

*<sup>a)</sup> Corresponding author: federica.bonomo@ipp.mpg.de*

**Abstract.** The ELISE test facility is based on a modular concept design which has been replicated in the ITER Negative Beam Ion (NBI) source with twice the size in the vertical direction. The target of ELISE is to achieve simultaneously the ITER NBI parameters in terms of negative ion extracted current (in H and D), pulse duration and ratio of co-extracted electron to ion below 1 at a source filling pressure of 0.3 Pa. While the source plasma can be operated for 1 h, only 9.5 s of beam extraction every  $\approx 150$  s can be applied, with a maximum total voltage of 60 kV due to limitations of the HV power supply; only divergences larger than 1 deg have been measured so far. The beam in ELISE is investigated by various diagnostics: the currents in the grid system are electrically measured and provide the total extracted negative ion current as well as information on the beam losses separately measured in the top and bottom grid segments of the extraction and grounded grids; the Beam Emission Spectroscopy (BES) gives information on the beam intensity and divergence (vertical and horizontal profiles); Infra-red (IR) analysis of the diagnostic calorimeter provides a 2D map of the beam power density and, consequently, the accelerated current density distribution as well as the total accelerated current. The spatial resolution of the beam diagnostics at ELISE (BES; diagnostic calorimeter) allows to resolve and describe in intensity and divergence the two beam segments associated to the two top and bottom grid segments. Following the evolution of the beam segments during the Cs conditioning process (i.e. Cs evaporation in the source to move from volume production of negative ions to surface production) allows to optimize the Cs conditioning by using the beam as an indirect measurement of the negative ion production. At high source performance and stable conditioning, the vertical beam uniformity in terms of accelerated current can be easily achieved: the difference between top and bottom beam segments is almost always well within the 10%.

## A LARGE UNIFORM NEGATIVE ION BEAM FOR ITER

Each of the two ITER heating and current drive (H&CD) neutral beam injection (NBI) systems must provide 16.5 MW of 1 MeV  $D_0$  (or 870 keV of  $H_0$ ) to the plasma [1]. The high beam energy is required to obtain deep enough penetration of the beam into the plasma and produce current drive, as well as to maximize the power per injector. The fast neutrals to be injected into the plasma originate from negative ions produced in a large source (approximately  $2\text{ m} \times 1\text{ m}$ ), coupled to an extraction system and several acceleration grids. The reference design for the ITER NBI grid system is based on the multi-aperture multi-grid (MAMuG) type electrostatic accelerator [1]: 1280 circular apertures are arranged in 16 rectangular beamlet groups, four for each of the four grid segments; the total extraction area is  $0.2\text{ m}^2$  [3]. The beamlets of each aperture merge to a large beam, with an accelerated negative ion current density of  $200\text{ A/m}^2$  for  $D^-$  and  $230\text{ A/m}^2$  for  $H^-$  (i.e. 40 A of total accelerated current in D and 46 A in H). The accelerated negative ions will be then neutralized by passing through a gas cell (neutralizer): collisions of the negative ions with the background gas create fast neutrals by stripping the outer electron with an efficiency of about 60 %. After removing the residual ions and electrons in the last part of the beam line by a residual ion dump, the fast neutrals will be injected into the ITER tokamak or hit a calorimeter. When injected into the tokamak, the fast neutrals will be ionized through collisions with plasma particles, thus transferring their energy to the plasma.

In order to maximize the beam efficiency and to minimize the heat loads on the grids and the components along the beamline as well as inside the duct close to the tokamak, the beam core divergence is required to be small (less than 0.4 deg for each beamlet [1]). The small divergence has to be combined with a beam uniformity better than 90 % (in terms of power density) to ensure a good transmission through the beam-line and a proper energy

deposition into the plasma. To minimize the losses along the beam line and limit the beamline component power loads, the source filling pressure has been set up to 0.3 Pa, at which the amount of stripped particles (i.e. portion of particles neutralized in the grid system before reaching the full energy) will be smaller than 30 % [1].

The ITER Neutral Beam Test Facility (PRIMA [4]) is located at Consorzio RFX (Padova, Italy). It includes two experimental devices: a 100 kV-extraction full-size ion source (SPIDER [5]) which has recently started the first experiments, and a full beam power (1 MV) full-size neutral beam injector (MITICA [3]). The main goal of SPIDER is to achieve the ITER-relevant extracted and accelerated currents in a full ITER-size source for pulse duration up to 1 hour; the main target of MITICA is to demonstrate the simultaneous achievement of all the operational parameters of the ITER NBI accelerator.

In the European roadmap towards the ITER NBI, a fundamental intermediate step is represented by the ELISE test facility, operating at IPP Garching since 2013 [6]. ELISE is equipped with a half-ITER-size negative ion source and has the target to demonstrate the possibility to achieve the ITER parameters in terms of currents (extracted and accelerated negative ions in hydrogen and deuterium) as well as co-extracted electrons at the operational filling pressure of 0.3 Pa, for pulses up to 1 hour in deuterium. At the moment, ELISE is the only test facility producing an ITER-relevant large negative ion beam (half-size of the ITER one in the vertical direction). The beam can be analyzed by several beam diagnostics, which are described in detail in the next section.

In this paper, the attention is focused on the vertical uniformity of the large ELISE beam in hydrogen operation during the caesium (Cs) conditioning procedure of the source (caesium is evaporated into the source in order to enhance the production of negative ions on a low work function surface). The beam diagnostic tools allow to measure the beam properties and to follow their evolution during the whole conditioning procedure. This starts in a Cs-free source (i.e. volume operation): the negative hydrogen ions are created by the dissociative attachment of electrons with hydrogen molecules at high vibrational state. To increase the amount of extracted negative ions, it is convenient to move from the volume to the surface production, which is based on the negative hydrogen ion formation by picking up the electrons from a surface (i.e. plasma grid). This process can be enhanced by lowering the work function of the surface by a thin layer of caesium, which is evaporated directly into the source [7]. The transition from volume to surface production in hydrogen has been monitored, until reaching a status of good conditioning, which permits to extract the largest amount of negative ions while simultaneously keeping the ratio of co-extracted electron to ion below 1. The procedure lasted 14 operational days (about 700 hundred plasma pulses for a total plasma-on time of about 9 h); the conditioning was carried out with the potential rods inside the source for the first time [8]. This conditioning procedure allowed to achieve the ELISE target for hydrogen operation, both in terms of accelerated currents and in pulse length (1000 s). In this paper, the focus is on the evolution of the beam properties during the transition from volume to surface production of negative ions for short pulses, i.e. 9.5 s of beam extraction within 20 s of plasma pulse, as well as on the attempt to produce a uniform large beam at the highest extracted ion current.

## THE ELISE TEST FACILITY AND THE BEAM DIAGNOSTICS

The ELISE test facility is the intermediate step between the RF driven ITER prototype source developed at IPP (extraction area of typically  $6 \times 10^{-3} \text{ m}^2$ ) [2] and the ion source for the ITER NBI system (extraction area of  $0.2 \text{ m}^2$ ) [1]. The design of the ion source and the extraction system is as close as possible to the ITER design but with some differences due to technical limitations or for enabling diagnostic access and a high experimental flexibility [6]. The original design has been modified in the last years as a consequence of optimization for high RF power and long pulses operation, which allowed to achieve the ITER NBI targets in hydrogen [8]. Among them: improved cooling of the electro-magnetic screens around the drivers to reduce mutual inductances; Teflon coating of a pair coils, introduction of silicon rubber fixation combs and substitution of driver alumina cylinders with quartz ones to reduce electric field strength at triple points and thus eliminate electric breakdowns [9]; solid state RF generators instead of oscillators [10]; external magnets to change the topology of the magnetic field in proximity of the extraction grid system [11].

In ELISE, plasma is generated in four drivers by inductive RF coupling (RF power  $\leq 75 \text{ kW/driver}$ ); the plasma then spreads into a rectangular expansion region. In order to minimize the amount of co-extracted electrons, a magnetic filter field (FF) is created by a current (IPG) flowing through the Plasma Grid (PG) [12] in combination with external permanent magnets [11]. A positive bias potential of the PG with respect to the source body and a bias plate at source potential surrounding the grid aperture groups, helps in the co-extracted electron reduction: the bias potential influences the plasma potential close to the PG, resulting in a plasma sheath attracting or repelling negative

particles onto the PG [13]. In ELISE, the bias potential is controlled by the current ( $I_{bias}$ ) flowing onto the bias plate, and not by the potential itself: this operational scenario is beneficial for obtaining stable operation [11]. To further modify the potential profile close to the PG, potential rods have been introduced in the source, in vertical direction in between the beamlet groups and close to the PG [14]; an optimal configuration has been identified by electrically connecting the potential rods to the PG.

The interplay between the magnetic field and the electric field in front of the PG causes a vertical plasma drift, which is upward for the standard filter field configuration [15]; external magnets change the magnetic field topology at the lateral sides of the extraction grids. On the beam side, the presence of the magnetic filter field causes a vertical beam deflection, which is downward directed for the field created solely by the IPG current. The amplitude of the beam deflection depends on the strength of the filter field in combination with the total acceleration voltage; in general it is on the average around 5-10 cm at the position of the calorimeter for extraction voltages in the range 5-7 kV, as shown by IR analysis of the power deposited at the calorimeter.

Once the electrons are co-extracted, they are deflected and dumped onto the second grid, the extraction grid (EG), by permanent magnets embedded into it to avoid their acceleration to full potential. This electron-suppression magnetic field causes also a small horizontal deflection of the negative ion beamlets; the field is such that the horizontal deflection is alternated (right-left) row by row among the apertures: the whole beam then travels toward the calorimeter, and is larger in horizontal direction due to the alternated beamlet deflection.

In ELISE, caesium is evaporated inside the source via two ovens with liquid caesium reservoirs, located in the middle of the lateral sides of the expansion chamber: it is evaporated towards the back-plate and then re-distributed mostly by the plasma itself [16]. In the extraction phase of the beam, the Cs re-distribution from the back of the source body towards the grids is enhanced by the back-streaming ions hitting the back-plate [16].

ELISE is designed to extract a large negative ion current using a three-grid extraction system with a ITER-like aperture geometry; the distances between plasma and extraction grid are the same as for SPIDER (and the maximum extraction voltage will be also the same, 10 kV) while the gap between EG and GG is in ELISE smaller than for SPIDER (15 mm instead of 35 mm). The total acceleration voltage is limited to 60 kV. So far, only divergences

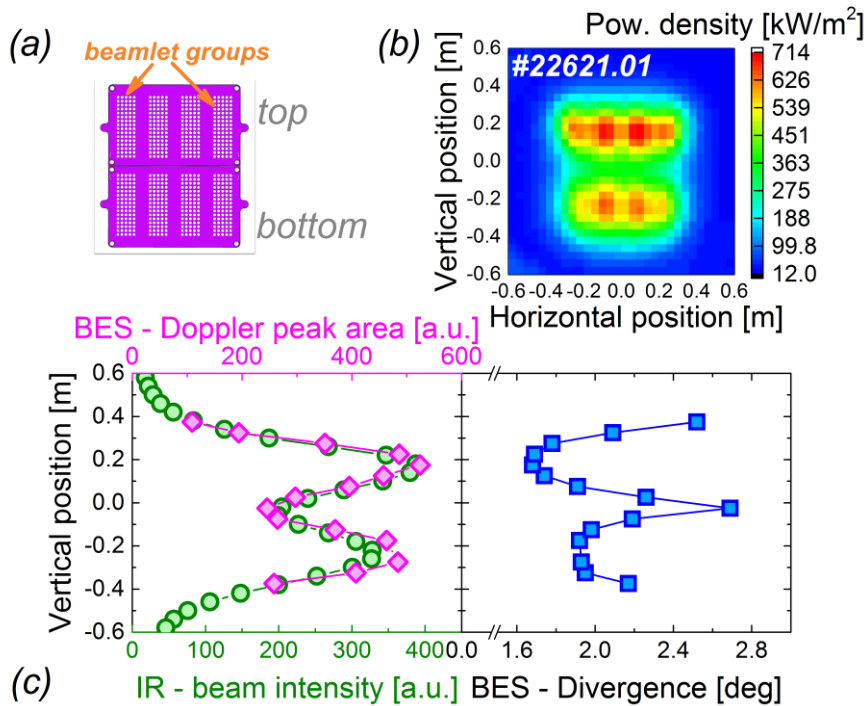


**FIGURE 1.** (a) Scheme of the ELISE grid system: two grid segments with 4 beamlet groups each. (b) Contour plot of the beam power deposited on the diagnostic calorimeter for the pulse #22621 (0.3 Pa,  $U_{HV} = 6$  kV + 30 kV), as detected by IR camera and (c) Left: vertical profiles of the beam intensity on the diagnostic calorimeter (green circles: values integrated over horizontal lines) and of the BES diagnostic (purple diamonds); Right: vertical profile of the beam divergence from BES (blue squares).

larger than 1 deg have been measured. The extraction system is in the vertical direction half of the ITER one: it consists in 640 extraction apertures arranged into eight rectangular beamlet groups, four for each grid segment (top and bottom) [6]. An image of the grid aperture scheme and of their spatial distribution is shown in FIGURE 1(a).

To analyze the large beam, several beam diagnostic tools have been implemented. The first beam diagnostic consists in the electrical measurements of the currents, providing the total extracted negative ion beam current ( $I_{ex}$ ) and the current ( $I_{EG}$ ) flowing through the extraction grid, mainly due to the co-extracted electrons; the two segments of the EG are electrically insulated to provide the  $I_{EG}$  current separately for the two segments (top and

bottom). The current flowing through the grounded grid ( $I_{GG}$ ) is measured too, again separately for the top and bottom segments.

The accelerated beam is stopped 3.5 m downstream from the GG onto a diagnostic calorimeter which is 1.2 m  $\times$  1.2 m in size [17]. It is made of four copper plates, each with its own cooling circuit. Inlet and outlet water temperatures are measured to provide independent beam power measurements via water calorimetry of the four beam sectors. On the beam side, a pattern of 15  $\times$  15 copper blocks is attached to each of the copper plates. 48 thermocouples are embedded into as many blocks, to provide two vertical and two horizontal beam profile measurements. Further details on the whole system can be found in Ref. [17]. The blocks act as inertial beam dumps, providing a 2D image of the beam (matrix of 30  $\times$  30). A MoS<sub>2</sub> black coating has been applied on the beam-side block surfaces to increase the surface emissivity, to reduce reflections and therefore to facilitate temperature measurements by a IR camera located outside of the beam tank and looking at the calorimeter through a ZnSe window. The absolute calibration of the IR camera is obtained shot by shot by evaluating the average emission coefficient of the calorimeter plates coating (which is being modified with time due to beam sputtering). This is done by comparing the block temperature measured by the IR camera with the one obtained with the 48 thermocouples. An example of the 2D map of the beam power at the calorimeter is shown in FIGURE 1(b): for good beam optics, the eight beamlet groups are distinguishable; differences in beam power and beam optics between the beamlet groups can be quantitatively obtained via 2D fit of eight bi-dimensional gaussians [18], one for each beamlet group. Information on the four beamlet groups belonging to the same grid segment allows the estimation of the accelerated current separately for the top and bottom grid segments ( $I_{acc}^{top}$  and  $I_{acc}^{bot}$ ); they are addressed as top and bottom beam segments.

Between the grid system and the diagnostic calorimeter, the Beam Emission Spectroscopy (BES) diagnostic tool is located. BES is based on the analysis of the spectra of H $_{\alpha}$  or D $_{\alpha}$  Doppler-shifted peak produced by the interaction of the fast ions with the background gas. The optic heads collecting the light are arranged to form a vertical array of 16 horizontal lines of sight (LOS), equally spaced by 5 cm, and a horizontal array of four vertical LOS, each one intercepting the center of the beamlets group; they provide, respectively, a vertical and a horizontal profile. The LOS defined by the optic heads intercept the core of the beam 2.6 m from the GG with an angle of 50 deg. Further details on the BES diagnostic tool in ELISE can be found in Ref. [19]. The BES diagnostic provides, in a non-invasive way, essentially three pieces of information for each LOS. i) The beam divergence ( $\varepsilon$ ) is estimated from the width of the main Doppler peak of the fully accelerated particles (half of the e-folding width, corrected by the instrumental factor of the spectrometer and the geometrical characteristics of the view of observation [19]). ii) Information on the beam profiles can be obtained from the Doppler peak area for an absolutely calibrated set of LOS. iii) The estimation of the stripping losses is obtained from the spectrum in between the main Doppler peak and the unshifted H $_{\alpha}$ /D $_{\alpha}$  peak. This paper focusses on the beam properties as derived in i) and ii). An example of the vertical beam intensity profile from BES for the beam in FIGURE 1(b) is displayed in FIGURE 1(c) by purple diamonds; the profile with green circles corresponds instead to the vertical beam profile from IR data analysis of the diagnostic calorimeter; the agreement is very good despite the 90 cm distance between the two measurement locations. The vertical divergence profile measured by BES is shown too (blue squares).

## VOLUME OPERATION OF A LARGE BEAM

In a Cs-free source, the large beam mirrors the main features of the formation and extraction of negative ions as produced and destructed in the plasma volume. The amount of co-extracted electrons reaches the interlock limit of the extraction system (the interlock stops the beam extraction to avoid damage to the extraction grid onto which the co-extracted electrons are impinging) already for low extraction voltage or RF power; the electron to ion ratio can be very high, above 100. Therefore, a large filter field in front of the PG as well as a high bias potential are needed to keep the amount of co-extracted electrons at a tolerable level. For the experiments here considered, the magnetic FF has been set at about 4 mT in front of the PG (as a result of the combination of the  $I_{PG}$  current flowing through the PG and the external magnets in the strengthening configuration [11]) and the bias potential  $U_{bias}$  at about 30-33 V ( $I_{bias}$  current controlled, set at 55 A). These values are much larger than those usually needed for hydrogen operation in a caesiated source. On the one hand they are essential for the reduction of the co-extracted electrons, on the other hand the combination of such a large magnetic field with the electric one creates a very strong vertical plasma drift in front of the PG, directed upward. The plasma positive ion density (measured by the Langmuir double probes positioned at 2 cm from the PG, in front of the two grid segments, one on the top and one in the bottom [20]) is larger (almost double) in front of the top grid segment than in front of the bottom one as for a caesiated

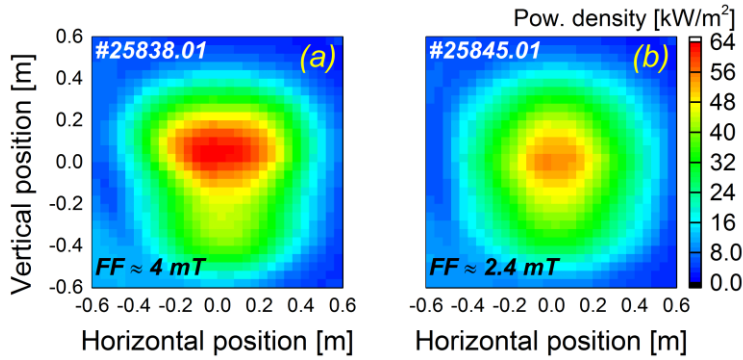


**FIGURE 2.** Volume operation: power density map for a high (a) and a low (b) magnetic filter field (0.3 Pa, 25 kW/driver,  $U_{HV}=3\text{kV}+20\text{kV}$ ).

beam segment than at the bottom one. The vertical non-uniformity changes with the intensity of the filter field: at smaller filter field intensity the beam becomes vertically more symmetric and centered, as displayed in FIGURE 2(b) for a filter field of about 2.4 mT; the top/bottom ratio of the positive ion density in front of the PG decreases from 1.7 of the case of FIGURE 2(a) to 1.2 for the case of FIGURE 2(b). In the latter case, the beam seems to be centered with respect to the calorimeter (highest intensity at the center of the calorimeter), however this is not the case: the presence of the filter field causes a downward deflection of the beam and as a result the beam intensity peak should be positioned well below the center of the calorimeter. That means that in the case of FIGURE 2(b), a higher amount of negative ions is still extracted from the top grid segment.

A further reduction of the FF in front of the PG to get a more uniform beam is not possible: the amount of co-extracted electrons would increase so much to damage the EG. An alternative way to improve the vertical beam uniformity in presence of a filter field could be to increase the current extracted from the bottom beam segment by increasing the RF power in the drivers which are illuminating that part of the grid. Increasing the RF power only in the bottom generator, the total extracted current  $I_{ex}$  increases as well, but the beam shape at the calorimeter does not change: the top beam segment continues to be much more intense than the bottom one. It has been found no top/bottom combination of RF power allowing for a vertically uniform beam during volume operation. The maximum RF power applied to the bottom drivers for this investigation was 42 kW/driver; for higher values the amount of co-extracted electrons would have been too high.

In volume operation, the estimation of a beam divergence from BES is not straightforward, as only the spectra collected from the vertical LOS show a Doppler shifted peak with almost gaussian shape (non-gaussian tails are always present); the horizontal LOS, instead, have a very large peak which looks like a double-peak in most of the cases. An example of such spectra is displayed in FIGURE 3: the gaussian peak from the vertical LOS is much narrower than from the horizontal LOS. As a consequence, the beam divergence (around 3.5 – 4 deg in volume) can be estimated only from the vertical LOS.

The presence of a double peak in the horizontal LOS is not due to the beam broad component (i.e. the part of the beam with a larger divergence) observed in Ref. [22], because it is not present in the vertical LOS. A possible explanation is a combination of very bad divergence (more than 3 deg from the vertical LOS) with the horizontal alternated (left-right) deflection of the negative ions due to the electron deflection field by the permanent magnets embedded into the EG. The row-by-row alternated horizontal deflection is probably seen by the BES diagnostic as the superposition of two different Doppler-shifted peaks; the two Gaussian peaks are very close one to the other due to the small deflection of the two populations of particles. Details on the impact of

source [20,21]. A higher positive ion density on top is correlated to a higher production of negative ions in the plasma volume, so that a larger amount of negative ions can be extracted there. An example of the beam power density map at the calorimeter for volume operation with a large filter field (about 4 mT) is displayed in FIGURE 2(a). The beam optics is not good enough to distinguish the single beamlet groups which are considerably overlapping. Nevertheless the vertical non-uniformity is clearly visible: a higher power density is produced at the top

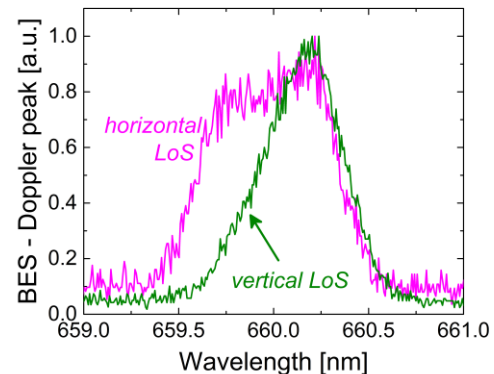


**FIGURE 3.** BES diagnostic in volume operation: Doppler peak spectrum for a horizontal and a vertical LOS. The horizontal LOS has a very large peak which looks like the superposition of two gaussian peaks.

different contributions to the width of the Doppler peak in a BES diagnostic can be found in Ref. [23].

## BEAM FEATURES DURING CS CONDITIONING

The ELISE beam can be used as a diagnostic tool for the status of conditioning of the source, being the direct result of the formation and extraction of the negative ions. For the Cs conditioning process starting from a Cs-free source, operational parameters are usually kept constant to observe and investigate the conditioning process, e.g. using a high filter field and bias potential to adequately reduce the co-extracted electrons. Only later on, when the amount of Cs in the source and on the plasma grid is large enough, and co-extracted electron currents are low, these parameters can be re-adjusted to achieve higher accelerated negative ion current.

In FIGURE 4(a), the first 14 days of the Cs conditioning process are displayed (about 700 pulses): a continuous evaporation of Cs into the source while repeating the beam pulses every 3-7 minutes. The total extracted negative ion current (red circles) increases from 2-3 A to 29 A while the ratio of co-extracted electrons over ions (green diamonds) drops from 30 (in volume) to less than 1 in the first two days; further small variations are due to daily/weekly conditioning of the source or parameter scans. In the first part of the initial phase (first 300 pulses of FIGURE 4(a), marked with a dashed line), all the operational settings and beam optics parameters have been kept constant ( $FF = 4$  mT,  $I_{bias} = 55$  A,  $U_{HV} = 5$  kV + 30 kV); afterwards they have been slightly adjusted. Further parameter adjustments for higher performances have been carried out later on (second phase in FIGURE 4(a)), but always for conditioning of short pulses. The whole procedure has taken 14 operational days to reach the ITER-relevant ion current for hydrogen [8].

During Cs conditioning, an increase in the accelerated current of the top segments is observed at first. An example of the beam power density map at the calorimeter after the first 300 pulses is displayed in FIGURE 4(b): the beam power density is higher in the top segment and the four beamlet groups are visible because of the lower divergence with respect to the beam bottom segment ( $div^{top}=2.5$  deg;  $div^{bot}=3.4$  deg). Only after further Cs conditioning (almost at the end of the conditioning phase of FIGURE 4(a)), it is possible to extract almost the same amount of current from both beam segments. Beam divergence is also similar (see FIGURE 4(c)). This is because the Cs redistribution is done by the plasma: a non-symmetric plasma density in front of the grid system causes a non-symmetric redistribution of the Cs onto the PG. More plasma pulses are then needed to re-distribute Cs on the bottom grid segments, to be able to extract and accelerate the same amount of ion current for both beam segments [16].

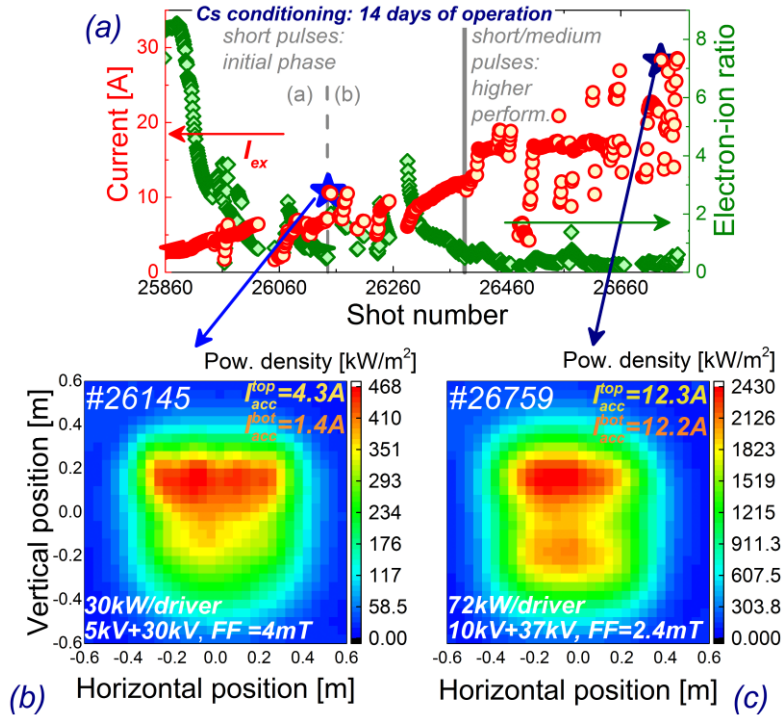


**FIGURE 4.** Cs conditioning phase – first month: (a) Evolution in time of the total extracted current  $I_{ex}$  (red circles) and of the ratio of co-extracted electrons over ions (green diamonds). (b) Beam power density map at the calorimeter after the first 300 pulses and (c) at the end of the Cs conditioning phase.

amount of current from both beam segments. Beam divergence is also similar (see FIGURE 4(c)). This is because the Cs redistribution is done by the plasma: a non-symmetric plasma density in front of the grid system causes a non-symmetric redistribution of the Cs onto the PG. More plasma pulses are then needed to re-distribute Cs on the bottom grid segments, to be able to extract and accelerate the same amount of ion current for both beam segments [16].

The different time-scale of Cs redistribution of top and bottom beam segments is confirmed also by the BES diagnostic. The increase of the extracted negative ion current at fixed extraction and acceleration voltages corresponds to a decrease of the beam divergence as expected considering the divergence-perveance correlation in under-perveant conditions [24], typically experienced in ELISE. This phenomenon occurs also during the transition from volume to surface

negative ion production, as shown in FIGURE 5: the full width at half maximum (FWHM) of the Doppler-shifted peak, almost proportional to the beam divergence, of a top BES LOS (blue triangles) decreases while the total extracted current  $I_{ex}$  (red circles) is increasing due to the Cs evaporation inside the source. For a bottom LOS (pink triangles) of FIGURE 5, the trend is similar but with two differences: the reduction of the peak FWHM starts later and the slope is smaller. At the end of the first part of the conditioning phase (right side of FIGURE 5) the Doppler-shifted peak FWHM for the bottom LOS is still larger than for the top one and it stays larger almost up to the end of the conditioning phase, shown in FIGURE 4(a). The whole Cs conditioning process is needed for extracting and accelerating almost the same amount of current from both the grid segments, with similar divergences.

The decrease of Doppler shifted peak FWHM in FIGURE 5 for the two horizontal LOS is actually a combination of two factors: the increase of extracted ion current and the disappearing of the “double gaussian peak” described in the previous paragraph and shown in FIGURE 3. The latter occurs gradually and with different time scales for the two beam segments: for the top LOS the double peak vanishes (or at least it cannot be detected any longer by the BES diagnostic) in 50 - 60 pulses while for the bottom LOS about 150 pulses are needed. The transition from a “double gaussian” peak to a typical Gaussian Doppler shifted peak is highlighted in FIGURE 5 by a star for each LOS. From then on, the peak FWHM decrease is due only to the increase of the extracted ion current.

The merging of the two Gaussian peaks into a single one when the source is caesiated, can be due to the different origin of the negative ions during the transition from volume to the surface production. In volume production, ions enter the extraction region from the volume of the expansion chamber (laminar flow) and they are influenced by the electron deflection field (around 7 mT at the plasma-facing side of the PG and up to 30 mT at the beam-facing side of the PG) so that their entrance angle into the aperture is horizontally deflected and alternated row by row. In a caesiated source, part of the negative ions is directly extracted from the chamfered surfaces of the plasma side of the PG, as described by the PIC Montecarlo ONIX code for a domain around a single aperture [25]: the influence of the electron deflection field is expected to be smaller for these particles. Some insights could be gained by coupling the ONIX simulations together with the particle tracking beam code BBC-NI [23] for the BES spectra simulation; investigations and modeling are ongoing work but a straightforward and clear explanation is still missing.

## UNIFORMITY OF A LARGE BEAM

Once the Cs conditioning process for short pulses is finished, the focus is on the optimization of the vertical beam uniformity. In ELISE, there are no diagnostics at the moment that could provide information on of the single beamlet intensity and divergences; the uniformity optimization can be done only “globally” in terms of the following quantities measured for the two beam segments: the accelerated ion current ( $I_{acc}^{top}$  and  $I_{acc}^{bot}$ ) provided by the IR analysis of the diagnostic calorimeter and the beam divergence ( $div^{top}$  and  $div^{bot}$ ) obtained by the BES diagnostic.

In terms of accelerated current at the calorimeter, the top/bottom beam uniformity is usually larger than 90 %, as displayed also in FIGURE 4(c), at the end of the Cs conditioning phase. Small differences in the top/bottom accelerated currents can be adjusted by changing the top/bottom RF power ratio. This technique was not successful during volume operation because of the large vertical plasma drift due to the strong FF; in a well caesiated source instead, it permits a fine tuning of the accelerated current separately for the two beam segments. At the highest performance, with a FF of about 2.5 mT, the ratio between the top and bottom RF power is about 0.9. Different magnetic configuration of the FF could require a different ratio.

Even though the accelerated currents for the top and bottom beam segments usually differ less than 10 %, most of the time the bottom beam segment seems to have less power density (as in FIGURE 4(c)): this is only an optical

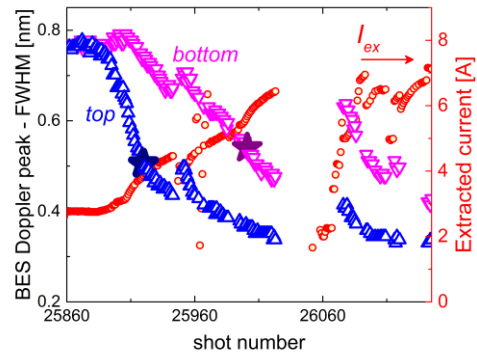


**FIGURE 5.** Initial phase of Cs conditioning at constant parameters and BES diagnostic: time evolution of the Doppler peak FWHM for two horizontal LOS in correspondence to the top (blue triangles) and bottom (purple triangles) beam segments; the total extracted current  $I_{ex}$  is displayed too (red circles).

effect due to a slightly worse divergence of the bottom beam segment with respect to the top one. An investigation on how to minimize the difference in terms of beam divergence for the two grid segments is ongoing.

## SUMMARY

In volume operation, the beam in the ELISE test facility is vertically non-uniform, due to the large upward plasma drift caused by the very intense filter field in front of the PG, which is nevertheless necessary to keep at a tolerable level the amount of co-extracted electrons. No compensation of the vertical beam non-uniformity is possible by RF power.

During the Cs conditioning process, the large beam of ELISE is used as a direct diagnostic of the status of the source conditioning. Its main features directly reflect the status of the Cs distribution at the PG, giving hints on how to continue with the conditioning procedure, e.g. top/bottom asymmetries give the operator information on how to adjust the Cs evaporation. In ELISE, but more in general as foreseen for the ITER NBI sources, redistribution of Cs is done essentially by the plasma and there is no direct control of the Cs distribution onto the PG.

Caesiation is faster on the top grid segment, where the plasma density is higher, than in the bottom one. During the conditioning phase, plasma density reaches comparable values in front of both PG segments, which improves the Cs conditioning also for the bottom segment. As soon as the amount of Cs is large enough on both PG segments, an increase of the accelerated ion current in the bottom beam segment is observed by the beam diagnostic tools.

Once good source performance and stable caesiation for short pulses is achieved, the beam uniformity can be further improved: uniformity of accelerated ion currents better than 90 % for top and bottom beam segments can be easily obtained in normal operation; fine adjustments can be carried out by a different RF power setting in the drivers. It is instead not possible at the moment to obtain similar beam divergences for the two beam segments and this topic needs further investigation.

## REFERENCES

1. R Hemsworth, D. Boilson, P. Blatchford et al, New J. Phys. **19**, 025005, (2017).
2. E. Speth et al., Nucl. Fusion **46**, S220 (2006).
3. P. Agostinetti et al., Nucl. Fusion **56**, 016015 (2016).
4. V. Toigo et al., Nucl. Fusion **55**, 083025 (2015).
5. V. Toigo et al., Nucl. Fusion **57**, 086027 (2017).
6. B. Heinemann et al., Fusion Engineering and Design **84**, 915–922 (2009).
7. B.S. Lee and M. Seidl, Appl. Phys. Lett. **61** 2857R (1992).
8. D. Wunderlich et al, *this conference*.
9. B. Heinemann et al., Fusion Engineering and Design, published online on 28<sup>th</sup> March 2018 (2018).
10. W. Kraus, D. Wunderlich, U. Fantz, Rev. Sci. Instrum. **89**, 052102 (2018).
11. D. Wunderlich, et al., Plasma Phys. Control. Fusion **58**, 125005 (2016).
12. M. Fröschle, et al., Fusion Eng. Des. **88**, 1015 (2013).
13. C. Wimmer, U. Fantz and the NNBI Team, J. Appl. Physics **12**, 073301 (2016).
14. W. Kraus et al., Rev. Sci. Instrum. **89**, 052102 (2018).
15. D. Wunderlich, U. Fantz, P. Franzen, R. Riedl, and F. Bonomo, Rev. Sci. Instrum. **84**, 093102 (2013).
16. A. Mimo, C. Wimmer, D. Wunderlich, and U. Fantz, AIP Conference Proceedings **1869**, 030019 (2017).
17. R. Nocentini et al., Fusion Engineering and Design **88**, 913– 917 (2013).
18. I. Mario, “*IR thermography analysis of the powerful hydrogen beam at ELISE*”, Master Thesis, Università degli Studi di Padova (2016).
19. B. Ruf, “*Reconstruction of Negative Hydrogen Ion Beam Properties from Beamline Diagnostics*”, Ph.D. thesis, Universität Augsburg, 2015.
20. C. Wimmer, I. Mario, U. Fantz and the NNBI team, *this conference*
21. U. Fantz, L. Schiesko, D. Wunderlich and the NNBI Team, AIP Proceedings **1515**, 187 (2013).
22. M. Barbisan, F. Bonomo, U. Fantz and D. Wunderlich, Plasma Phys. Control. Fusion **59**, 055017 (2017).
23. A. Hurlbatt, F. Bonomo, D. Wuenderlich, U. Fantz and the NNBI Team, *this conference*.
24. P. Franzen, U. Fantz, and the NNBI Team, AIP Conference Proceedings **1390**, 310 (2011).
25. A. Revel, et al., Journal of Appl. Physics **122**, 103302 (2017).